LUND UNIVERSITY

Fisher information integral operator and spectral decomposition for inverse scattering problems

Nordebo, Sven; Fhager, Andreas; Gustafsson, Mats; Nilsson, Börje

2009

Link to publication

Citation for published version (APA):
Nordebo, S., Fhager, A., Gustafsson, M., & Nilsson, B. (2009). *Fisher information integral operator and spectral decomposition for inverse scattering problems*. (Technical Report LUTEDX/(TEAT-7180)/1-21/(2009)). [Publisher information missing].

Total number of authors:
4

General rights
Unless other specific re-use rights are stated the following general rights apply:
Copyright and moral rights for the publications made accessible in the public portal are retained by the authors and/or other copyright owners and it is a condition of accessing publications that users recognise and abide by the legal requirements associated with these rights.
• Users may download and print one copy of any publication from the public portal for the purpose of private study or research.
• You may not further distribute the material or use it for any profit-making activity or commercial gain
• You may freely distribute the URL identifying the publication in the public portal

Read more about Creative commons licenses: https://creativecommons.org/licenses/

Take down policy
If you believe that this document breaches copyright please contact us providing details, and we will remove access to the work immediately and investigate your claim.

LUND UNIVERSITY

PO Box 117
221 00 Lund
+46 46-222 00 00

Download date: 19. Dec. 2025

CODEN:LUTEDX/(TEAT-7180)/1-21/(2009)

Fisher information integral operator and spectral decomposition for inverse scattering problems

Sven Nordebo, Andreas Fhager, Mats Gustafsson, and Börje Nilsson

Electromagnetic Theory
Department of Electrical and Information Technology
Lund University
Sweden

Sven Nordebo
sven.nordebo@msi.vxu.se

School of Mathematics and Systems Engineering
Växjö University
SE-351 95 Växjö
Sweden

Andreas Fhager
elfad@chalmers.se

Department of Signals and Systems
Chalmers University of Technology
SE-412 96 Göteborg
Sweden

Mats Gustafsson
Mats.Gustafsson@eit.lth.se

Department of Electrical and Information Technology
Electromagnetic Theory
Lund University
P.O. Box 118
SE-221 00 Lund
Sweden

Börje Nilsson
borje.nilsson@msi.vxu.se

School of Mathematics and Systems Engineering
Växjö University
SE-351 95 Växjö
Sweden

Editor: Gerhard Kristensson
© Sven Nordebo *et al.*, Lund, June 23, 2009

Abstract

The purpose of this paper is to introduce the Fisher information integral operator and related spectral decomposition for inverse scattering problems. The Fisher information integral kernel is derived using a variational formulation and Fréchet derivatives leading naturally to a first order perturbation analysis of the partial differential equation at hand, and an application of corresponding Green's function techniques. The integral operator and its spectrum can be efficiently approximated by using suitable quadrature methods for numerical integration. The eigenfunctions of this integral operator, corresponding to the identifiable parameters via the significant eigenvalues and the corresponding Cramér-Rao bounds, constitute a suitable global basis for sensitivity and resolution analysis as well as for optimization. In depth analysis and numerical examples for one- and two-dimensional inverse electromagnetic scattering problems are given that illustrate the spectral decomposition and the related resolution analysis.

1 Introduction

Inverse scattering problems offer many challenges in related sciences due to the ill-posedness of the reconstruction, see *e.g.*, [2, 9, 11, 26]. Important technical application areas are *e.g.*, with microwave tomography [6, 7], non-invasive medical imaging [13], and electrical impedance tomography [3]. In these applications, it is almost always necessary to employ some kind of regularization to stabilize the inversion algorithms and there is only a limited resolution attainable, see *e.g.*, [2, 8, 11, 18, 21].

The Fisher information and the Cramér-Rao bound are very useful tools for resolution and sensitivity analysis in various signal estimation and imaging problems based on wave physics, see *e.g.*, [4, 5, 8, 16, 18–20, 25, 27]. With inverse scattering problems, the Fisher information is able to connect a parameter based description of the material with a physical model, together with some probabilistic assumption about the measurement errors. The Gaussian assumption, which is a simple and yet realistic model for the measurement errors, yields a statistical bound for the estimation errors, and hence a quantitative measure on the inversion quality, see *e.g.*, [8, 16, 18]. In [8, 18–20], the Cramér-Rao bound is employed as an analytical tool to quantify the ill-posedness of the reconstruction and to explicitely describe the inherent trade-off between the accuracy and the resolution, and in [17] the Fisher information is used in a preconditioning strategy to improve the convergence properties of a gradient based inversion algorithm.

The purpose of this paper is to introduce the Fisher Information integral Operator (FIO) and related spectral decomposition for inverse scattering problems. So far, the Fisher information analysis presented in [8, 17, 18] has been finite dimensional by presumption. Hence, the analysis has been suffering from the necessity and related uncertainty of making ad hoc a priori assumptions about the underlying discretization of the material such as the size, orientation and positions of the assumed image pixels, etc. An infinite dimensional formulation with FIO analysis will completely circumvent this drawback. There is furthermore a distinct computational advantage

of using the infinite dimensional formulation in the related spectral analysis since the eigenvalues and eigenfunctions of the integral operator can be approximated by employing efficient quadrature methods for numerical integration [14] instead of using an excessively small a priori discretization grid in the finite dimensional formulation.

Spectral analysis of linear integral operators are well known tools in mathematical analysis [14], inverse scattering [2, 11, 21] as well as in random process characterization [24, 28]. The Fisher information integral operator for an infinite dimensional parameter function has been employed previously in the estimation of wave forms (or random processes) in *e.g.*, [28]. In the present context with inverse problems, the Fisher information integral kernel is derived using a variational formulation and Fréchet derivatives leading naturally to a first order perturbation analysis of the partial differential equation at hand, and an application of corresponding Green's function techniques.

The in depth analysis and numerical examples are concerned with one- and two-dimensional inverse electromagnetic scattering problems based on the Helmholtz equation and related free space Green's functions. For the one-dimensional problem the integral kernel have some similarities with the Dirichlet kernel and related prolate spheriodal wave (eigen) functions [24, 28]. For the two-dimensional problem with circular symmetry, an azimuthal Fourier series expansion efficiently separates the two-dimensional eigenproblem into several one-dimensional problems, one for each Fourier component.

The organization of the paper is as follows. The Fisher information integral operator for inverse scattering problems is introduced in section 2. In depth analysis of one- and two-dimensional inverse electromagnetic scattering problems are treated in sections 3 and 4, respectively. Section 5 contains the numerical examples and section 6 the summary.

2 The Fisher information integral operator

2.1 Variational formulation of the Fisher information

The Fisher Information integral Operator (FIO) is a natural extension of the corresponding Fisher Information Matrix (FIM), and can hence be derived in close resemblance to the development given in *e.g.*, [10]. Let $\theta = \theta(\boldsymbol{r})$ denote the unknown real valued parameter function to be estimated, defined on a compact spatial domain Ω. Let $\theta \in \mathcal{D}[\Omega]$ where $\mathcal{D}[\Omega]$ denotes the space of piecewise continuous functions on Ω.

Let $\boldsymbol{\xi} \in \mathbb{C}^n$ denote a finite vector of complex valued sample measurements, modeled as a random vector with conditional probability density function $p(\boldsymbol{\xi}|\theta)$. To obtain the infinite dimensional Fisher information kernel, a first order perturbation analysis is considered. Let $\delta\mathcal{T}$ denote the Fréchet derivative of an operator $\mathcal{T}$ with respect to an incremental parameter function $\delta\theta \in \mathcal{D}[\Omega]$, see *e.g.*, [11]. In particular, assume that the function $F(h) = \ln p(\boldsymbol{\xi}|\theta + h\delta\theta)$ is differentiable in the real variable h, *i.e.*, $F(h) = F(0) + F'(0)h + \mathcal{O}\{h^2\}$ where $(\cdot)'$ denotes differentiation with respect to

h. The Fréchet derivative (*cf.*, the first variation) of $\ln p(\boldsymbol{\xi}|\theta)$ can then be calculated as $\delta \ln p(\boldsymbol{\xi}|\theta) = F'(0)$. Hence, it is straightforward to see that *e.g.*, $\delta \ln p(\boldsymbol{\xi}|\theta) = \delta p(\boldsymbol{\xi}|\theta)/p(\boldsymbol{\xi}|\theta)$. Moreover, since the Fréchet derivative is a linear operator, it has a representation of the form

$$\delta \ln p(\boldsymbol{\xi}|\theta) = \langle \delta_{\theta(\boldsymbol{r})} \ln p(\boldsymbol{\xi}|\theta), \delta\theta(\boldsymbol{r}) \rangle = \int_{\Omega} \delta_{\theta(\boldsymbol{r})} \ln p(\boldsymbol{\xi}|\theta) \delta\theta(\boldsymbol{r}) \, \mathrm{d}v, \tag{2.1}$$

where $\langle \cdot, \cdot \rangle$ denotes a scalar product over Ω and $\delta_{\theta(\boldsymbol{r})} \ln p(\boldsymbol{\xi}|\theta)$ the corresponding gradient [11], *cf.*, also the Riesz representation theorems for linear functionals [23].

Consider now an unbiased estimator $\hat{\theta}(\boldsymbol{r}, \boldsymbol{\xi})$ with

$$\mathcal{E}\left\{\hat{\theta}(\boldsymbol{r}, \boldsymbol{\xi})\right\} = \int \hat{\theta}(\boldsymbol{r}, \boldsymbol{\xi}) p(\boldsymbol{\xi}|\theta) \, \mathrm{d}\boldsymbol{\xi} = \theta(\boldsymbol{r}), \tag{2.2}$$

where $\mathcal{E}\{\cdot\}$ denotes the expectation operator with respect to the conditional probability density function $p(\boldsymbol{\xi}|\theta)$. Taking the Fréchet derivative of both sides of (2.2) with respect to $\delta\theta$ yields

$$\delta\mathcal{E}\left\{\hat{\theta}(\boldsymbol{r}, \boldsymbol{\xi})\right\} = \int \hat{\theta}(\boldsymbol{r}, \boldsymbol{\xi}) \delta \ln p(\boldsymbol{\xi}|\theta) p(\boldsymbol{\xi}|\theta) \, \mathrm{d}\boldsymbol{\xi} = \mathcal{E}\left\{\hat{\theta}(\boldsymbol{r}, \boldsymbol{\xi}) \delta \ln p(\boldsymbol{\xi}|\theta)\right\} = \delta\theta(\boldsymbol{r}), \tag{2.3}$$

where it has been assumed that the variational operator δ commutes with the integral. Furthermore, by employing the regularity condition $\mathcal{E}\{\delta \ln p(\boldsymbol{\xi}|\theta)\} = \mathcal{E}\{\delta p(\boldsymbol{\xi}|\theta)/p(\boldsymbol{\xi}|\theta)\} = \int \delta p(\boldsymbol{\xi}|\theta) \, \mathrm{d}\boldsymbol{\xi} = \delta 1 = 0$ (employing that the variational operator δ commutes with the integral), it is concluded that

$$\mathcal{E}\left\{\left(\hat{\theta}(\boldsymbol{r}, \boldsymbol{\xi}) - \theta(\boldsymbol{r})\right) \delta \ln p(\boldsymbol{\xi}|\theta)\right\} = \delta\theta(\boldsymbol{r}). \tag{2.4}$$

Now, let $a(\boldsymbol{r}) \in \mathcal{D}[\Omega]$ and $b(\boldsymbol{r}) \in \mathcal{D}[\Omega]$ be arbitrary (test) functions. Let $\delta\theta(\boldsymbol{r}) = b(\boldsymbol{r})$ and take the scalar product $\langle a(\boldsymbol{r}), \cdot \rangle$ of both sides of (2.4) yielding

$$\mathcal{E}\left\{\langle a(\boldsymbol{r}), \hat{\theta}(\boldsymbol{r}, \boldsymbol{\xi}) - \theta(\boldsymbol{r}) \rangle \langle \delta_{\theta(\boldsymbol{r})} \ln p(\boldsymbol{\xi}|\theta), b(\boldsymbol{r}) \rangle\right\} = \langle a(\boldsymbol{r}), b(\boldsymbol{r}) \rangle, \tag{2.5}$$

where the scalar product $\langle a(\boldsymbol{r}), \cdot \rangle$ is assumed to commute with the expectation operation. The Cauchy-Schwarz inequality for stochastic variables [10] yields

$$\langle a(\boldsymbol{r}), b(\boldsymbol{r}) \rangle^2 \leq \mathcal{E}\left\{\langle a(\boldsymbol{r}), \hat{\theta}(\boldsymbol{r}, \boldsymbol{\xi}) - \theta(\boldsymbol{r}) \rangle^2\right\} \mathcal{E}\left\{\langle \delta_{\theta(\boldsymbol{r})} \ln p(\boldsymbol{\xi}|\theta), b(\boldsymbol{r}) \rangle^2\right\}. \tag{2.6}$$

By defining the following integral kernels

$$\mathcal{C}(\boldsymbol{r}', \boldsymbol{r}'') = \mathcal{E}\left\{\left(\hat{\theta}(\boldsymbol{r}', \boldsymbol{\xi}) - \theta(\boldsymbol{r}')\right)\left(\hat{\theta}(\boldsymbol{r}'', \boldsymbol{\xi}) - \theta(\boldsymbol{r}'')\right)\right\} \tag{2.7}$$

$$\mathcal{I}(\boldsymbol{r}', \boldsymbol{r}'') = \mathcal{E}\left\{\delta_{\theta(\boldsymbol{r}')} \ln p(\boldsymbol{\xi}|\theta) \delta_{\theta(\boldsymbol{r}'')} \ln p(\boldsymbol{\xi}|\theta)\right\} \tag{2.8}$$

and the corresponding covariance and Fisher information integral operators $\mathcal{C}$ and $\mathcal{I}$

$$\mathcal{C}a(\boldsymbol{r}) = \int_{\Omega} \mathcal{C}(\boldsymbol{r}, \boldsymbol{r}') a(\boldsymbol{r}') \, \mathrm{d}v', \tag{2.9}$$

$$\mathcal{I}b(\boldsymbol{r}) = \int_{\Omega} \mathcal{I}(\boldsymbol{r}, \boldsymbol{r}') b(\boldsymbol{r}') \, \mathrm{d}v', \tag{2.10}$$

the Cauchy-Schwarz inequality (2.6) finally yields

$$\langle a(\boldsymbol{r}), b(\boldsymbol{r})\rangle^2 \leq \langle a(\boldsymbol{r}), \mathcal{C}a(\boldsymbol{r})\rangle\langle b(\boldsymbol{r}), \mathcal{I}b(\boldsymbol{r})\rangle, \tag{2.11}$$

where it has been assumed that the expectation operator commutes with the integrals.

2.2 Cramér-Rao bound for the principal parameters

It is assumed that the operator $\mathcal{I}$ is compact and self-adjoint, with an associated discrete spectrum *cf.*, [14]. Consider the following eigenvalue problem

$$\mathcal{I}\vartheta_l(\boldsymbol{r}) = \int_\Omega \mathcal{I}(\boldsymbol{r}, \boldsymbol{r}')\vartheta_l(\boldsymbol{r}')\,\mathrm{d}v' = \mu_l\vartheta_l(\boldsymbol{r}) \tag{2.12}$$

where $\boldsymbol{r} \in \Omega$ and where $\mu_l > 0$ is a positive eigenvalue, $\vartheta_l(\boldsymbol{r}) \in \mathcal{D}[\Omega]$ the corresponding normalized eigenfunction and l a countable index. Similar to the Karhunen-Loève expansion of a stochastic process [28], the principal parameters η_l and the corresponding unbiased estimator $\hat{\eta}_l(\boldsymbol{\xi})$ are defined here by

$$\eta_l = \langle \theta(\boldsymbol{r}), \vartheta_l(\boldsymbol{r})\rangle = \int_\Omega \theta(\boldsymbol{r})\vartheta_l(\boldsymbol{r})\,\mathrm{d}v \tag{2.13}$$

$$\hat{\eta}_l(\boldsymbol{\xi}) = \langle \hat{\theta}(\boldsymbol{r}, \boldsymbol{\xi}), \vartheta_l(\boldsymbol{r})\rangle = \int_\Omega \hat{\theta}(\boldsymbol{r}, \boldsymbol{\xi})\vartheta_l(\boldsymbol{r})\,\mathrm{d}v. \tag{2.14}$$

By choosing $a(\boldsymbol{r}) = \vartheta_l(\boldsymbol{r})$ and $b(\boldsymbol{r}) = \frac{1}{\mu_l}\vartheta_l(\boldsymbol{r})$ in (2.11) and by noting that $\langle \vartheta_l(\boldsymbol{r}), \mathcal{C}\vartheta_l(\boldsymbol{r})\rangle = \mathcal{E}\{(\hat{\eta}_l(\boldsymbol{\xi}) - \eta_l)^2\}$, the Cramér-Rao bound for the principal parameters are given by

$$\mathcal{E}\{(\hat{\eta}_l(\boldsymbol{\xi}) - \eta_l)^2\} \geq \frac{1}{\mu_l}. \tag{2.15}$$

2.3 The Gaussian measurement model

Let $(\cdot)^{\mathrm{T}}$ and $(\cdot)^{\mathrm{H}}$ denote the transpose and the conjugate transpose, respectively. Consider the following Gaussian measurement model

$$\boldsymbol{\xi} = \boldsymbol{\psi}(\theta) + \boldsymbol{N} \tag{2.16}$$

where $\boldsymbol{\xi} \in \mathbb{C}^n$ is the complex measurement vector, $\boldsymbol{\psi}(\theta) \in \mathbb{C}^n$ a complex vector valued functional of the real function $\theta(\boldsymbol{r})$ and $\boldsymbol{N} \in \mathbb{C}^n$ a complex Gaussian random vector with zero mean and covariance matrix $\mathcal{E}\{\boldsymbol{N}\boldsymbol{N}^{\mathrm{H}}\} = \mathbf{R}$, see *e.g.*, [10]. Hence, the probability density function $p(\boldsymbol{\xi}|\theta)$ for the measurement vector is given by

$$p(\boldsymbol{\xi}|\theta) = \frac{1}{\pi^n \det\mathbf{R}} \mathrm{e}^{-(\boldsymbol{\xi}-\boldsymbol{\psi}(\theta))^{\mathrm{H}}\mathbf{R}^{-1}(\boldsymbol{\xi}-\boldsymbol{\psi}(\theta))}. \tag{2.17}$$

By employing the correlation properties of the complex Gaussian vector [10], *i.e.*, $\mathcal{E}\{(\boldsymbol{\xi} - \boldsymbol{\psi}(\theta))(\boldsymbol{\xi} - \boldsymbol{\psi}(\theta))^{\mathrm{H}}\} = \mathbf{R}$ and $\mathcal{E}\{(\boldsymbol{\xi} - \boldsymbol{\psi}(\theta))(\boldsymbol{\xi} - \boldsymbol{\psi}(\theta))^{\mathrm{T}}\} = \mathbf{0}$, it is straightforward to show that (2.8) becomes

$$\mathcal{I}(\boldsymbol{r}', \boldsymbol{r}'') = 2\,\mathrm{Re}\left\{\delta_{\theta(\boldsymbol{r}')}\boldsymbol{\psi}^{\mathrm{H}}(\theta)\mathbf{R}^{-1}\delta_{\theta(\boldsymbol{r}'')}\boldsymbol{\psi}(\theta)\right\}. \tag{2.18}$$

2.4 Continuous measurements over time and frequency

Consider the following statistical measurement model regarding a single spatial measurement point,

$$\xi(t) = \psi(t,\theta) + N(t),\ t \in [-T/2, T/2] \tag{2.19}$$

where $\xi(t)$ is the real time-domain stochastic measurement process, $\psi(t,\theta)$ the physical observation model, $N(t)$ the noise and T the length of the observation interval. The noise is assumed to be sampled from a real Gaussian stochastic process with zero mean, correlation function $r_{\mathrm{N}}(\tau) = \mathcal{E}\{N(t+\tau)N(t)\}$ and power spectral density $R_{\mathrm{N}}(f) = \int_{-\infty}^{\infty} r_{\mathrm{N}}(\tau)\mathrm{e}^{\mathrm{i}2\pi f\tau}\,\mathrm{d}\tau$.

The complex Hilbert pair, or analytic signal[1] corresponding to (2.19) is given by

$$\tilde{\xi}(t) = \tilde{\psi}(t,\theta) + \tilde{N}(t),\ t \in [-T/2, T/2] \tag{2.20}$$

where $\tilde{N}(t)$ is zero mean complex Gaussian noise with power spectral density $\tilde{R}_{\mathrm{N}}(f) = 4R_{\mathrm{N}}(f)u(f)$ where $u(f)$ is the Heaviside unit step function, *cf.*, [10, 15, 22]. A discrete measurement model is now obtained from a Fourier series representation of (2.20)

$$\tilde{\xi}_p = \tilde{\psi}_p(\theta) + \tilde{N}_p,\ -\infty < p < \infty \tag{2.21}$$

where the Fourier coefficients are $\tilde{\xi}_p = \frac{1}{T}\int_{-T/2}^{T/2} \tilde{\xi}(t)\mathrm{e}^{\mathrm{i}2\pi\frac{p}{T}t}\,\mathrm{d}t$. The noise terms $\tilde{N}_p$ are zero mean complex Gaussian[2] with covariance function $\tilde{R}_{pq} = \mathcal{E}\{\tilde{N}_p\tilde{N}_q^*\}$, see *e.g.*, [28]. Provided that the correlation function $\tilde{r}_N(\tau)$ has either finite support or finite energy, it is straightforward to show that $\tilde{R}_{pq} \to \frac{1}{T}\tilde{R}_{\mathrm{N}}(\frac{p}{T})\delta_{pq}$ as $T \to \infty$ where δ_{pq} denotes the Kronecker delta, see *e.g.*, [12]. From (2.18) and (2.21) it is now concluded that

$$\begin{aligned}\mathcal{I}(\boldsymbol{r}',\boldsymbol{r}'') &= 2\,\mathrm{Re}\sum_{p=-\infty}^{\infty}\frac{1}{\tilde{R}_{\mathrm{N}}(\frac{p}{T})}\delta_{\theta(\boldsymbol{r}')}T\tilde{\psi}_p^*(\theta)\delta_{\theta(\boldsymbol{r}'')}T\tilde{\psi}_p(\theta)\frac{1}{T}\\ &\to 2\,\mathrm{Re}\int_{-\infty}^{\infty}\frac{1}{\tilde{R}_{\mathrm{N}}(f)}\delta_{\theta(\boldsymbol{r}')}\tilde{\psi}^*(f,\theta)\delta_{\theta(\boldsymbol{r}'')}\tilde{\psi}(f,\theta)\,\mathrm{d}f\\ &= 2\,\mathrm{Re}\int_{0}^{\infty}\frac{1}{R_{\mathrm{N}}(f)}\delta_{\theta(\boldsymbol{r}')}\psi^*(f,\theta)\delta_{\theta(\boldsymbol{r}'')}\psi(f,\theta)\,\mathrm{d}f\end{aligned} \tag{2.22}$$

as $T \to \infty$, and where the relations $\tilde{R}_{\mathrm{N}}(f) = 4R_{\mathrm{N}}(f)u(f)$ and $\tilde{\psi}(f,\theta) = 2\psi(f,\theta)u(f)$ have been used. Since $\psi(t,\theta)$ is real and $\psi(-f,\theta) = \psi^*(f,\theta)$, the Fisher information integral kernel is finally given by

$$\mathcal{I}(\boldsymbol{r}',\boldsymbol{r}'') = \int_{-\infty}^{\infty}\frac{1}{R_{\mathrm{N}}(f)}\delta_{\theta(\boldsymbol{r}')}\psi^*(f,\theta)\delta_{\theta(\boldsymbol{r}'')}\psi(f,\theta)\,\mathrm{d}f. \tag{2.23}$$

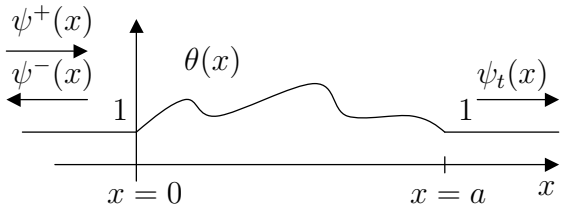

Figure 1: One-dimensional inverse scattering problem with a parameter function $\theta(x)$ over a finite interval $x \in [0, a]$.

3 One-dimensional inverse scattering

Consider the one-dimensional inverse scattering problem of imaging a parameter function $\theta(x)$ over a finite interval $x \in \Omega = [0, a]$ where $a > 0$ and $\theta(x) = 1$ for $x \notin [0, a]$, see Fig. 1. The inverse scattering problem may be acoustic or electromagnetic, etc. For an electromagnetic problem the parameter function may be *e.g.*, $\theta(x) = \epsilon(x)/\epsilon$ where $\epsilon(x)$ denotes the relative permittivity inside a dielectric slab and ϵ its value outside. It is assumed that the wave field $\psi(x)$ satisfies the Helmholtz equation in the frequency domain

$$\partial_x^2 \psi(x) + k^2 \theta(x) \psi(x) = 0 \tag{3.1}$$

where $k = \omega/c$ is the wave number, $\omega = 2\pi f$ the angular frequency with time convention $\mathrm{e}^{-\mathrm{i}\omega t}$ and c the speed of wave propagation in the surrounding medium where $\theta(x) = 1$. The boundary conditions consist of an incident wave field $\psi^+(x) = S(f)\mathrm{e}^{\mathrm{i}kx}$, a reflected wave field $\psi^-(x) = S(f)\Gamma(f)\mathrm{e}^{-\mathrm{i}kx}$ for $x \leq 0$ and a transmitted wave field $\psi_t(x) = S(f)T(f)\mathrm{e}^{\mathrm{i}kx}$ for $x \geq a$ where $\Gamma(f)$ and $T(f)$ denote the reflection and the transmission coefficients, respectively, and $S(f)$ the Fourier transform of the excitation signal. The inverse problem consists of retrieving the parameter function $\theta(x)$ based on a measurement of the scattered field $\psi^-(x)$ at the boundary $x = 0$ over some fixed frequency range.

For a low contrast inverse scattering problem it is of interest to analyze the situation for a homogenous background where $\theta(x) = 1$ for all x. The solution to (3.1) with boundary conditions is then simply $\psi(x) = \psi^+(x) = S(f)\mathrm{e}^{\mathrm{i}kx}$. The corresponding Green's function satisfies $\partial_x^2 G(x, x') + k^2 G(x, x') = -\delta(x - x')$ and is given by $G(x, x') = \frac{\mathrm{i}}{2k}\mathrm{e}^{\mathrm{i}k|x-x'|}$.

3.1 The sensitivity field and Fisher information

To obtain the sensitivity field $\delta_{\theta(x)}\psi = \delta_{\theta(\boldsymbol{r})}\psi$ used in (2.23), a first order perturbation analysis is considered in (3.1) where $\theta(x) \to \theta(x) + h\delta\theta(x)$ and $\psi(x) \to \psi(x) + h\delta\psi(x) + \mathcal{O}(h^2)$ where $\delta\theta(x) \in \mathcal{D}[\Omega]$ and $\|\mathcal{O}(h^2)\| \leq Ch^2$ as $h \to 0$. The resulting

[1] The analytic time-domain signal is $\tilde{\xi}(t) = \xi(t) + \mathrm{i}\check{\xi}(t)$ where $\check{\xi}(t)$ denotes the Hilbert transform, see *e.g.*, [22].

[2] Note that the Fourier series representation of a real Gaussian process is not necessarily complex Gaussian, *cf.*, [10, 15, 28].

non-homogenous wave equation for the Fréchet derivative $\delta\psi(x)$ is

$$\partial_x^2\delta\psi(x) + k^2\theta(x)\delta\psi(x) = -k^2\psi(x)\delta\theta(x) \tag{3.2}$$

where $\psi(x)$ is given by the solution to (3.1). Note that the boundary conditions in (3.2) are given by $\delta\psi^+(x) = 0$. The solution to (3.2) is given by

$$\delta\psi(x) = \int_\Omega G(x,x')k^2\psi(x')\delta\theta(x')\,\mathrm{d}x' \tag{3.3}$$

and the corresponding gradient is obtained as

$$\delta_{\theta(x')}\psi(x) = G(x,x')k^2\psi(x'). \tag{3.4}$$

Consider a homogenous background with $\theta(x) = 1$ for all x, and suppose that the observed quantity $\psi(f,\theta)$ in (2.23) is the reflection data in the present formulation, *i.e.*, the wave field $\psi(x)$ observed at the boundary $x = 0$. Hence,

$$\delta_{\theta(x')}\psi(f,\theta) = \delta_{\theta(x')}\psi(x)|_{x=0} = k^2G(0,x')\psi(x') = \frac{\mathrm{i}k}{2}S(f)\mathrm{e}^{\mathrm{i}k2x'}. \tag{3.5}$$

Suppose further that we wish to evaluate (2.23) over a bandwidth $\omega \in \omega_0[1 - B/2, 1 + B/2]$ where ω_0 is the center frequency and B the normalized bandwidth with $0 < B \leq 2$. Suppose also that the excitation signal $S(f)$ as well as the power spectral density $R_\mathrm{N}(f)$ are constant over the relevant bandwidth, *i.e.*, $S(f) = S$ and $R_\mathrm{N}(f) = N_0$. The Fisher information integral kernel in (2.23) then becomes

$$\mathcal{I}(x',x'') = \mathrm{SNR}k_0^2\frac{1}{B}\,\mathrm{Re}\int_{1-B/2}^{1+B/2}\nu^2\mathrm{e}^{\mathrm{i}\nu 2k_0(x''-x')}\,\mathrm{d}\nu \tag{3.6}$$

where $k_0 = \omega_0/c$, $\nu = \omega/\omega_0$ and where the dimensionless signal to noise ratio SNR is defined by

$$\mathrm{SNR} = \frac{1}{2N_0}\,\mathrm{Re}\int_{f_0(1-B/2)}^{f_0(1+B/2)}|S(f)|^2\,\mathrm{d}f = \frac{f_0B}{2N_0}|S|^2. \tag{3.7}$$

For simplicity, we choose $\mathrm{SNR} = 1$ in the following. It is also convenient to consider the dimensionless Fisher information, defined with respect to the normalized spatial variable k_0x

$$\mathcal{I}(k_0x',k_0x'') = \frac{1}{B}\,\mathrm{Re}\int_{1-B/2}^{1+B/2}\nu^2\mathrm{e}^{\mathrm{i}\nu 2(k_0x''-k_0x')}\,\mathrm{d}\nu. \tag{3.8}$$

By employing the Fourier transform relationship $(\mathrm{i}\nu)^2 \leftrightarrow \frac{\partial^2}{\partial z^2}$ (where $z = 2(k_0x'' - k_0x')$), the Fisher information in (3.8) is finally given by

$$\mathcal{I}(k_0x',k_0x'') = -\frac{1}{4}\frac{\partial^2}{\partial x^2}\left\{\cos 2x\frac{\sin Bx}{Bx}\right\}\Bigg|_{x=k_0(x''-x')}. \tag{3.9}$$

Note that the kernel defined in (3.9) is continuous, and the corresponding operator $\mathcal{I}$ is hence compact and self-adjoint, *cf.*, [14].

3.2 The eigenvalue problem

Consider now the eigenvalue problem (2.12) with normalized Fisher information as in (3.8) and (3.9), *i.e.*,

$$\int_0^{k_0 a} g(x-x')\vartheta_l(x')\,\mathrm{d}x' = \mu_l \vartheta_l(x) \tag{3.10}$$

where the normalization $x \leftrightarrow k_0 x$ has been used, and where

$$\begin{aligned} g(x) &= -\frac{1}{4}\frac{\partial^2}{\partial x^2}\left\{\cos 2x \frac{\sin Bx}{Bx}\right\} \\ &= \frac{\cos 2x \cos Bx}{2x^2} + \frac{\cos Bx \sin 2x}{x} - \frac{\cos 2x \sin Bx}{2Bx^3} \\ &\quad + \frac{\cos 2x \sin Bx}{Bx} + \frac{B\cos 2x \sin Bx}{4x} - \frac{\sin 2x \sin Bx}{Bx^2}. \end{aligned} \tag{3.11}$$

Hence, $\mathcal{I}(k_0 x', k_0 x'') = g(k_0(x'-x''))$, and the dimensionless eigenvalues and eigenfunctions corresponding to (3.10) are $\mu_l^{\mathrm{norm}} = \mu_l/k_0$ and $\vartheta_l^{\mathrm{norm}}(k_0 x) = \frac{1}{\sqrt{k_0}}\vartheta_l(x)$, respectively, where μ_l and $\vartheta_l(x)$ are defined in (2.12). It is also noted that $g(x) = g(-x)$ and $g(0) = 1 + B^2/12$.

It is observed that the kernel function (3.11) is a continuous analogue of the Fisher information for the corresponding discrete multilayer slab [8]. It is also observed that (3.11) is a modulated analogue of the well-known Dirichlet kernel with related prolate spheriodal eigenfunctions [24, 28].

To solve the eigenvalue problem (3.10) numerically, any suitable quadrature method for one-dimensional numerical integration [14] can be used. Thus, an approximate finite dimensional matrix formulation can be employed

$$\boldsymbol{\mathcal{I}}\boldsymbol{\vartheta}_l = \mu_l \boldsymbol{\vartheta}_l, \tag{3.12}$$

where $\boldsymbol{\mathcal{I}}$ is $N \times N$, $\boldsymbol{\vartheta}_l$ is $N \times 1$ and N the number of quadrature points.

3.3 Asymptotic analysis

The Fourier transform of $g(x)$ in (3.11) is

$$G(\nu) = \int_{-\infty}^{\infty} g(x)\mathrm{e}^{\mathrm{i}\nu x}\,\mathrm{d}x = \begin{cases} \frac{\pi}{8B}\nu^2 & |\nu \pm 2| \le B \\ 0 & \text{otherwise.} \end{cases} \tag{3.13}$$

As $k_0 a \to \infty$, the eigenvalues and eigenfunctions of (3.10) are asymptotically,

$$\mu_l \sim G(l\frac{2\pi}{k_0 a}),\ -\infty < l < \infty \tag{3.14}$$

$$\vartheta_l(x) \sim \frac{1}{\sqrt{k_0 a}}\mathrm{e}^{\mathrm{i}l\frac{2\pi}{k_0 a}x},\ 0 \le x \le k_0 a \tag{3.15}$$

see *e.g.*, [28]. Note that $G(\nu)$ is real and symmetric, so that $\mu_l = \mu_{-l}$ and $\vartheta_l(x) = \vartheta_{-l}^*(x)$.

Asymptotically, the number of nonzero eigenvalues are

$$N = \frac{4B}{\frac{2\pi}{k_0 a}} = \frac{2B}{\pi} k_0 a \tag{3.16}$$

and the normalized resolution $\Delta\{k_0 x\}$ is

$$\Delta\{k_0 x\} = \frac{k_0 a}{N} = \frac{\pi}{2B}. \tag{3.17}$$

The spatial resolution Δx is therefore given by

$$\Delta x = \frac{\pi}{2k_0 B} = \frac{\lambda_0}{4B} \geq \frac{\lambda_0}{8} \tag{3.18}$$

where $\lambda_0 = 2\pi/k_0$ is the wavelength corresponding to the center frequency and $0 < B \leq 2$.

Alternatively, using the minimum wavelength $\lambda_{\min} = \lambda_0/(1 + B/2)$, the spatial resolution in (3.18) becomes

$$\Delta x = \frac{\lambda_{\min}}{4B}(1 + \frac{B}{2}) \geq \frac{\lambda_{\min}}{4}. \tag{3.19}$$

4 Two-dimensional inverse scattering

Consider the two-dimensional electromagnetic inverse scattering problem of imaging an isotropic circular cylinder of radius a in a homogenous and isotropic background space, see Fig. 2. Let (ρ, ϕ, z) denote the cylindrical coordinates, $(\hat{\boldsymbol{\rho}}, \hat{\boldsymbol{\phi}}, \hat{\boldsymbol{z}})$ the corresponding unit vectors and $\boldsymbol{\rho} = \rho\hat{\boldsymbol{\rho}}$ the two-dimensional radius vector with coordinates (ρ, ϕ). Let $\theta = \theta(\boldsymbol{\rho})$ denote the unknown real valued function to be estimated, defined on the compact two-dimensional spatial domain $\Omega = \{\boldsymbol{\rho} | \rho \leq a\}$ where $a > 0$, see Fig. 2.

Both the electric field field $\boldsymbol{E}$ and the excitation (line) source $\boldsymbol{J}$ are assumed to be linearly polarized with $\boldsymbol{E} = \psi(\boldsymbol{\rho}, t)\hat{\boldsymbol{z}}$ and $\boldsymbol{J} = J(\boldsymbol{\rho}, t)\hat{\boldsymbol{z}}$, and both fields depend on the two-dimensional spatial domain $\boldsymbol{\rho} \in \mathbb{R}^2$. The measurement is performed on a cylinder of radius b with near-field excitation at (b, φ) and measurement at (b, ϕ). The inverse problem consists of estimating the parameter function $\theta(\boldsymbol{\rho}) = \epsilon(\boldsymbol{\rho})/\epsilon$ within the cylindrical object for $\rho \leq a$, based on measurements (or observations) of the electric field $\psi(\phi, \varphi, t) = \psi(\boldsymbol{\rho}, t)$ at $\rho = b$, *i.e.*, for $(\phi, \varphi, t) \in [0, 2\pi] \times [0, 2\pi] \times [-T/2, T/2]$ where T is the length of the observation interval. Here, $\epsilon(\boldsymbol{\rho})$ is the relative permittivity within the cylinder, and ϵ its value outside. Hence, $\theta(\boldsymbol{\rho}) = 1$ for $\rho > a$.

In the frequency domain, the Maxwell's equations yield the following wave equation for the scalar field ψ, *i.e.*, the Helmholtz equation in cylindrical coordinates

$$\nabla^2\psi(\boldsymbol{\rho}) + k^2\theta(\boldsymbol{\rho})\psi(\boldsymbol{\rho}) = \left\{\frac{1}{\rho}\frac{\partial}{\partial\rho}\rho\frac{\partial}{\partial\rho} + \frac{1}{\rho^2}\frac{\partial^2}{\partial\phi^2} + k^2\theta(\boldsymbol{\rho})\right\}\psi(\boldsymbol{\rho}) = -\mathrm{i}k\eta J(\boldsymbol{\rho}), \tag{4.1}$$

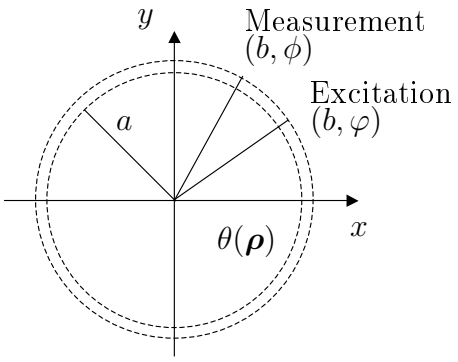

Figure 2: Two-dimensional inverse scattering problem with a parameter function $\theta(\boldsymbol{\rho})$ over a cylinder $\rho \leq a$. Measurement cylinder of radius $b > a$ with excitation at (b, φ) and measurement at (b, ϕ). The background space is homogenous and isotropic with $\theta(\boldsymbol{\rho}) = 1$ for $\rho > a$.

where $k = \omega/c$ is the wave number, $\omega = 2\pi f$ the angular frequency with the time convention $\mathrm{e}^{-\mathrm{i}\omega t}$, c the speed of wave propagation in the surrounding medium where $\theta(\boldsymbol{\rho}) = 1$ and η the corresponding wave impedance. The corresponding Green's function $G(\boldsymbol{\rho}, \boldsymbol{\rho}') = G(\rho, \phi, \rho', \phi')$ for a line source at $\boldsymbol{\rho}' = (\rho', \phi')$ satisfies $\{\nabla^2 \psi + k^2\theta\} G(\boldsymbol{\rho}, \boldsymbol{\rho}') = -\delta(\boldsymbol{\rho} - \boldsymbol{\rho}')$.

For a homogenous background with $\theta(\boldsymbol{\rho}) = 1$, the background Green's function is given by

$$G(\rho, \phi, \rho', \phi') = \frac{\mathrm{i}}{4} \sum_{m=-\infty}^{\infty} \mathrm{J}_m(k\rho_<)\mathrm{H}_m^{(1)}(k\rho_>)\mathrm{e}^{\mathrm{i}m(\phi-\phi')} \tag{4.2}$$

where $\mathrm{J}_m(\cdot)$ and $\mathrm{H}_m^{(1)}(\cdot)$ are the Bessel function and the Hankel function of the first kind, respectively, both of order m, see *e.g.*, [1]. Here, $\rho_< = \min\{\rho, \rho'\}$ and $\rho_> = \max\{\rho, \rho'\}$. Assuming that the source is a line source at $\boldsymbol{\rho}'$ with $J(\boldsymbol{\rho}) = S(f)\delta(\boldsymbol{\rho} - \boldsymbol{\rho}')$, the solution to (4.1) is given by

$$\psi(\boldsymbol{\rho}, f) = \int_{-\infty}^{\infty} \psi(\boldsymbol{\rho}, t)\mathrm{e}^{\mathrm{i}2\pi f t}\,\mathrm{d}t = \mathrm{i}k\eta S(f) G(\boldsymbol{\rho}, \boldsymbol{\rho}') \tag{4.3}$$

where $S(f)$ is the Fourier transform of the excitation signal. Hence, in the frequency domain, the observed field is given by $\psi(\phi, \varphi, f) = \psi(\boldsymbol{\rho}, f)|_{\rho=b} = \mathrm{i}k\eta S(f) G(b, \phi, b, \varphi)$. Further, let the two-dimensional Fourier coefficients of the $2\pi \times 2\pi$ periodic function $\psi(\phi, \varphi, f)$ be defined by

$$\psi_{mn}(f) = \frac{1}{(2\pi)^2} \int_0^{2\pi} \int_0^{2\pi} \psi(\phi, \varphi, f)\mathrm{e}^{-\mathrm{i}m\phi - \mathrm{i}n\varphi}\,\mathrm{d}\phi\,\mathrm{d}\varphi. \tag{4.4}$$

For the homogenous background, it follows then from (4.2) that
$\psi_{mn}(f) = -\frac{k\eta}{4} S(f)\mathrm{J}_m(kb)\mathrm{H}_m^{(1)}(kb)\delta_{-m,n}$.

4.1 Continuous measurements over time and space

Consider the following statistical measurement model for the space and time domain

$$\xi(\phi,\varphi,t) = \psi(\phi,\varphi,t) + N(\phi,\varphi,t) \tag{4.5}$$

for $(\phi,\varphi,t) \in [0,2\pi]\times[0,2\pi]\times[-T/2,T/2]$, which is a two-dimensional extension of the (single spatial point) model in (2.19), and where the argument θ in $\psi(\phi,\varphi,t)$ has been suppressed for simplicity. The measurement signal $\psi(\phi,\varphi,t)$ is assumed to be real and the noise $N(\phi,\varphi,t)$ is assumed to be sampled from a spatially uncorrelated real Gaussian stochastic process with zero mean and correlation function

$$\mathcal{E}\left\{N(\phi+\Delta\phi,\varphi+\Delta\varphi,t+\Delta t)N(\phi,\varphi,t)\right\} = (2\pi)^2\delta(\Delta\phi)\delta(\Delta\varphi)r_{\mathrm{N}}(\Delta t), \tag{4.6}$$

where $\delta(\cdot)$ denotes an impulse function with period 2π. Here, $r_{\mathrm{N}}(\tau)$ denotes the temporal correlation function with power spectral density $R_{\mathrm{N}}(f) = \int_{-\infty}^{\infty} r_{\mathrm{N}}(\tau)\mathrm{e}^{\mathrm{i}2\pi f\tau}\,\mathrm{d}\tau$. The complex (time-domain) Hilbert pair corresponding to (4.5) is given by

$$\tilde{\xi}(\phi,\varphi,t) = \tilde{\psi}(\phi,\varphi,t) + \tilde{N}(\phi,\varphi,t),\ t\in[-T/2,T/2] \tag{4.7}$$

where $\tilde{N}(\phi,\varphi,t)$ is a zero mean complex Gaussian stochastic process with the corresponding temporal power spectral density $\tilde{R}_{\mathrm{N}}(f) = 4R_{\mathrm{N}}(f)u(f)$, as in section 2.4. A discrete measurement model is obtained by considering the three-dimensional Fourier series representation of (4.7)

$$\tilde{\xi}_{mnp} = \tilde{\psi}_{mnp} + \tilde{N}_{mnp} \tag{4.8}$$

where the Fourier series coefficients are given by

$$\tilde{\xi}_{mnp} = \frac{1}{(2\pi)^2 T}\int_0^{2\pi}\int_0^{2\pi}\int_{-T/2}^{T/2}\tilde{\xi}(\phi,\varphi,t)\mathrm{e}^{-\mathrm{i}m\phi}\mathrm{e}^{-\mathrm{i}n\varphi}\mathrm{e}^{\mathrm{i}2\pi\frac{p}{T}t}\,\mathrm{d}t\,\mathrm{d}\phi\,\mathrm{d}\varphi. \tag{4.9}$$

Following the arguments as in section 2.4, it is straightforward to show that the noise terms $\tilde{N}_{mnp}$ are zero mean complex Gaussian distributed with covariance function

$$\mathcal{E}\left\{\tilde{N}_{mnp}\tilde{N}^*_{m'n'p'}\right\} = \delta_{mm'}\delta_{nn'}\frac{1}{T}\tilde{R}_{\mathrm{N}}(\frac{p}{T})\delta_{pp'} \tag{4.10}$$

as $T\to\infty$. Hence, from (2.18) with $\delta_{\theta(\boldsymbol{r}')} = \delta_{\theta(\boldsymbol{\rho}')}$, and the model (4.8), it follows that

$$\begin{aligned}
\mathcal{I}(\boldsymbol{\rho}',\boldsymbol{\rho}'') &= 2\,\mathrm{Re}\sum_{m=-\infty}^{\infty}\sum_{n=-\infty}^{\infty}\sum_{p=-\infty}^{\infty}\frac{1}{\tilde{R}_{\mathrm{N}}(\frac{p}{T})}\delta_{\theta(\boldsymbol{\rho}')}T\tilde{\psi}^*_{mnp}\delta_{\theta(\boldsymbol{\rho}'')}T\tilde{\psi}_{mnp}\frac{1}{T}\\
&\to 2\,\mathrm{Re}\int_{-\infty}^{\infty}\frac{1}{\tilde{R}_{\mathrm{N}}(f)}\sum_{m=-\infty}^{\infty}\sum_{n=-\infty}^{\infty}\delta_{\theta(\boldsymbol{\rho}')}\tilde{\psi}^*_{mn}(f)\delta_{\theta(\boldsymbol{\rho}'')}\tilde{\psi}_{mn}(f)\,\mathrm{d}f\\
&= 2\,\mathrm{Re}\int_{0}^{\infty}\frac{1}{R_{\mathrm{N}}(f)}\sum_{m=-\infty}^{\infty}\sum_{n=-\infty}^{\infty}\delta_{\theta(\boldsymbol{\rho}')}\psi^*_{mn}(f)\delta_{\theta(\boldsymbol{\rho}'')}\psi_{mn}(f)\,\mathrm{d}f
\end{aligned} \tag{4.11}$$

as $T \to \infty$, where the relations $\tilde{R}_{\mathrm{N}}(f) = 4R_{\mathrm{N}}(f)u(f)$ and $\tilde{\psi}_{mn}(f) = 2\psi_{mn}(f)u(f)$ have been used. Since $\psi(\phi, \varphi, t)$ is real and $\psi_{-m,-n}(-f) = \psi^*_{mn}(f)$, the Fisher information integral kernel is finally given by

$$\mathcal{I}(\boldsymbol{\rho}', \boldsymbol{\rho}'') = \int_{-\infty}^{\infty} \frac{1}{R_{\mathrm{N}}(f)} \sum_{m=-\infty}^{\infty} \sum_{n=-\infty}^{\infty} \delta_{\theta(\boldsymbol{\rho}')} \psi^*_{mn}(f) \delta_{\theta(\boldsymbol{\rho}'')} \psi_{mn}(f) \, \mathrm{d}f. \tag{4.12}$$

4.2 The sensitivity field

To obtain the sensitivity field used in (4.12), a first order perturbation analysis is considered in (4.1) where $\theta(\boldsymbol{\rho}) \to \theta(\boldsymbol{\rho}) + h\delta\theta(\boldsymbol{\rho})$ and $\psi(\boldsymbol{\rho}) \to \psi(\boldsymbol{\rho}) + h\delta\psi(\boldsymbol{\rho}) + \mathcal{O}(h^2)$ where $\delta\theta(\boldsymbol{\rho}) \in \mathcal{D}[\Omega]$ and $\|\mathcal{O}(h^2)\| \leq Ch^2$ as $h \to 0$. The resulting non-homogenous wave equation for the Fréchet derivative $\delta\psi(\boldsymbol{\rho})$ is

$$\nabla^2 \delta\psi(\boldsymbol{\rho}) + k^2 \theta(\boldsymbol{\rho}) \delta\psi(\boldsymbol{\rho}) = -k^2 \psi(\boldsymbol{\rho}) \delta\theta(\boldsymbol{\rho}) \tag{4.13}$$

where $\psi(\boldsymbol{\rho})$ is given by the solution to (4.1). The solution to (4.13) is given by

$$\delta\psi(\boldsymbol{\rho}) = \int_{\Omega} G(\boldsymbol{\rho}, \boldsymbol{\rho}') k^2 \psi(\boldsymbol{\rho}') \delta\theta(\boldsymbol{\rho}') \, \mathrm{d}S' \tag{4.14}$$

and the corresponding gradient is obtained as

$$\delta_{\theta(\boldsymbol{\rho}')} \psi(\boldsymbol{\rho}) = k^2 G(\boldsymbol{\rho}, \boldsymbol{\rho}') \psi(\boldsymbol{\rho}'). \tag{4.15}$$

Since the excitation is a line source at (b, φ) and $\psi(\boldsymbol{\rho}') = \mathrm{i}k\eta S(f) G(\rho', \phi', b, \varphi)$ as given by (4.3), the gradient of the observed field $\psi(\phi, \varphi, f)$ is

$$\delta_{\theta(\boldsymbol{\rho}')} \psi(\phi, \varphi, f) = k^3 \mathrm{i}\eta S(f) G(b, \phi, \rho', \phi') G(b, \varphi, \rho', \phi') \tag{4.16}$$

where the symmetry of the Green's function has been employed.

For a homogenous background with $\theta(\boldsymbol{\rho}) = 1$, the two-dimensional Fourier series representation of (4.16) follows by applying (4.2). Hence,

$$\delta_{\theta(\boldsymbol{\rho}')} \psi_{mn}(f) = -\frac{k^3 \mathrm{i}\eta S(f)}{16} J_m(k\rho') J_n(k\rho') H_m^{(1)}(kb) H_n^{(1)}(kb) \mathrm{e}^{-\mathrm{i}(m+n)\phi'}. \tag{4.17}$$

The Fisher information in (4.12) can now be expressed as

$$\mathcal{I}(\boldsymbol{\rho}', \boldsymbol{\rho}'') = \int_{-\infty}^{\infty} \frac{1}{R_{\mathrm{N}}(f)} \frac{k^6 \eta^2 |S(f)|^2}{16^2} \sum_{m=-\infty}^{\infty} \sum_{n=-\infty}^{\infty} J_m(k\rho') J_n(k\rho') J_m(k\rho'') J_n(k\rho'') \\ |H_m^{(1)}(kb)|^2 |H_n^{(1)}(kb)|^2 \mathrm{e}^{\mathrm{i}(m+n)(\phi' - \phi'')} \, \mathrm{d}f. \tag{4.18}$$

Next, suppose that the noise power spectral density and the excitation is constant over the relevant bandwidth, *i.e.*, $R_{\mathrm{N}}(f) = N_0$ and $\omega S(f) = \omega_0 S(f_0)$, respectively, for $\omega \in \omega_0[1 - B/2, 1 + B/2]$ where ω_0 is the center frequency and B the normalized

bandwidth. Further, let $\nu = \omega/\omega_0 = f/f_0 = k/k_0$ denote the normalized frequency variable, and define the dimensionless signal to noise ratio SNR by

$$\mathrm{SNR} = \frac{2}{N_0 16^2} \int_{f_0(1-B/2)}^{f_0(1+B/2)} k^2\eta^2 |S(f)|^2 \,\mathrm{d}f = \frac{2k_0^2\eta^2|S(f_0)|^2 f_0 B}{N_0 16^2}. \tag{4.19}$$

The Fisher information in (4.18) can then be expressed as

$$\mathcal{I}(\boldsymbol{\rho}', \boldsymbol{\rho}'') = \frac{\mathrm{SNR}}{B} k_0^4 \int_{1-B/2}^{1+B/2} \nu^4 \sum_{m=-\infty}^{\infty} \sum_{n=-\infty}^{\infty} J_m(\nu k_0 \rho') J_n(\nu k_0 \rho') J_m(\nu k_0 \rho'') J_n(\nu k_0 \rho'') \\ |H_m^{(1)}(\nu k_0 b)|^2 |H_n^{(1)}(\nu k_0 b)|^2 \mathrm{e}^{\mathrm{i}(m+n)(\phi'-\phi'')} \,\mathrm{d}\nu. \tag{4.20}$$

For simplicity, we choose SNR = 1 in the following. Finally, the Fisher information with respect to the dimensionless spatial variable $\boldsymbol{\rho} \leftrightarrow k_0\boldsymbol{\rho}$ is given by

$$\mathcal{I}(\boldsymbol{\rho}', \boldsymbol{\rho}'') = \frac{1}{B} \int_{1-B/2}^{1+B/2} \nu^4 \sum_{m=-\infty}^{\infty} \sum_{n=-\infty}^{\infty} J_m(\nu \rho') J_n(\nu \rho') J_m(\nu \rho'') J_n(\nu \rho'') \\ |H_m^{(1)}(\nu k_0 b)|^2 |H_n^{(1)}(\nu k_0 b)|^2 \mathrm{e}^{\mathrm{i}(m+n)(\phi'-\phi'')} \,\mathrm{d}\nu \tag{4.21}$$

and the corresponding dimensionless eigenvalues and eigenfunctions are $\mu_l^{\mathrm{norm}} = \mu_l/k_0^2$ and $\vartheta_l^{\mathrm{norm}}(k_0\boldsymbol{\rho}) = \frac{1}{k_0}\vartheta_l(\boldsymbol{\rho})$, respectively, where μ_l and $\vartheta_l(\boldsymbol{\rho})$ are defined in (2.12). Note that the kernel defined in (4.21) is continuous since $\rho', \rho'' \leq a < b$, *cf.*, also (4.16), and the operator $\mathcal{I}$ is hence compact and self-adjoint, *cf.*, [14]. It is also observed that the kernel function (4.21) is a continuous analogue of the Fisher information for the corresponding discretized circular domain presented in [18].

4.3 The eigenvalue problem

Due to the circular symmetry and a reorganization of the double summation, the Fisher information in (4.21) can be expressed as

$$\mathcal{I}(\rho', \rho'', \phi) = \sum_{q=-\infty}^{\infty} \mathcal{I}_q(\rho', \rho'') \mathrm{e}^{\mathrm{i}q\phi} \tag{4.22}$$

where $\phi = \phi' - \phi''$, and where the Fourier series coefficients in (4.22) are given by

$$\mathcal{I}_q(\rho', \rho'') = \frac{1}{B} \sum_{m=-\infty}^{\infty} \int_{1-B/2}^{1+B/2} \nu^4 J_m(\nu\rho') J_{q-m}(\nu\rho') J_m(\nu\rho'') J_{q-m}(\nu\rho'') \\ |H_m^{(1)}(\nu k_0 b)|^2 |H_{q-m}^{(1)}(\nu k_0 b)|^2 \,\mathrm{d}\nu. \tag{4.23}$$

Note that the Fourier series coefficients $\mathcal{I}_q(\rho', \rho'')$ are real and symmetric, *i.e.*, $\mathcal{I}_{-q}(\rho', \rho'') = \mathcal{I}_q(\rho', \rho'')$.

The eigenvalue problem in (2.12) can now be stated as

$$\int_{\rho \leq k_0 a} \int_0^{2\pi} \mathcal{I}(\rho, \rho', \phi - \phi') \vartheta_l(\rho', \phi') \,\mathrm{d}\phi' \rho' \,\mathrm{d}\rho' = \mu_l \vartheta_l(\rho, \phi) \tag{4.24}$$

or, equivalently, as the following Fourier series representation

$$2\pi \int_{\rho \le k_0 a} \mathcal{I}_q(\rho, \rho') \vartheta_{lq}(\rho') \rho' \, \mathrm{d}\rho' = \mu_l \vartheta_{lq}(\rho) \tag{4.25}$$

where $-\infty < q < \infty$, and

$$\vartheta_l(\rho, \phi) = \sum_{q=-\infty}^{\infty} \vartheta_{lq}(\rho) \mathrm{e}^{\mathrm{i}q\phi}. \tag{4.26}$$

Let q be arbitrary and fixed, and let $\vartheta_{lq}(\rho)$ be an eigenfunction of (4.25) with eigenvalue μ_l. Then $\vartheta_l(\rho, \phi) = \vartheta_{lq}(\rho)\mathrm{e}^{\mathrm{i}q\phi}$ is an eigenfunction of (4.24) with eigenvalue μ_l. Hence, since the integral operator $\mathcal{I}$ defined by (4.24) is compact and self-adjoint, the Fourier series representation in (4.26) is finite [14] (where the summation limits depend on l).

For $q = 0$, eigenvalues μ_l and eigenfunctions $\vartheta_l(\rho, \phi) = \widetilde{\vartheta}_{l0}(\rho)$ are generated where $\widetilde{\vartheta}_{l0}(\rho)$ are the corresponding real eigenfunction solutions of (4.25). Since the Fisher information is real with $\mathcal{I}_{-q}(\rho', \rho'') = \mathcal{I}_q(\rho', \rho'')$, any pair $(q, -q)$ with $q \ge 1$ will generate (at least) two linearly independent eigenfunctions $\vartheta_{lq}(\rho)\mathrm{e}^{\mathrm{i}q\phi}$ and $\vartheta_{l,-q}(\rho)\mathrm{e}^{-\mathrm{i}q\phi}$ sharing the corresponding eigenvalue μ_l. Real eigenfunctions (corresponding to the real parameter function $\theta(\rho, \phi)$) satisfying the conjugate symmetry $\vartheta_{l,-q}(\rho) = \vartheta_{lq}^*(\rho)$ are obtained as

$$\begin{cases} \vartheta_l^{\mathrm{a}}(\rho, \phi) = \widetilde{\vartheta}_{lq}(\rho)\mathrm{e}^{\mathrm{i}q\phi} + \widetilde{\vartheta}_{lq}(\rho)\mathrm{e}^{-\mathrm{i}q\phi} = 2\widetilde{\vartheta}_{lq}(\rho)\cos q\phi \\ \vartheta_l^{\mathrm{b}}(\rho, \phi) = -\mathrm{i}\widetilde{\vartheta}_{lq}(\rho)\mathrm{e}^{\mathrm{i}q\phi} + \mathrm{i}\widetilde{\vartheta}_{lq}(\rho)\mathrm{e}^{-\mathrm{i}q\phi} = 2\widetilde{\vartheta}_{lq}(\rho)\sin q\phi \end{cases} \tag{4.27}$$

where $\widetilde{\vartheta}_{lq}(\rho)$ are the real eigenfunction solutions of (4.25) for $q \ge 1$. The set of all eigenvalues and eigenfunctions of (4.24) may be obtained as the union of all the eigenvalues and eigenfunctions generated by (4.25) for $-\infty < q < \infty$, counted with multiplicity.

To solve the eigenvalue problem (4.24) numerically, let the Fourier series in (4.26) be truncated with $|q| \le Q$. Any suitable quadrature method for one-dimensional numerical integration [14] can now be used to approximate (4.25) using a finite dimensional matrix formulation given by

$$2\pi \boldsymbol{\mathcal{I}}_q \widetilde{\boldsymbol{\vartheta}}_{lq} = \mu_l \widetilde{\boldsymbol{\vartheta}}_{lq}, \;\; q = 0, \ldots, Q \tag{4.28}$$

where $\boldsymbol{\mathcal{I}}_q$ is $N \times N$, $\widetilde{\boldsymbol{\vartheta}}_{lq}$ is $N \times 1$ and N the number of quadrature points.

5 Numerical examples

5.1 One-dimensional inverse scattering

Consider the one-dimensional inverse scattering problem described in section 3. The dimensionless Fisher information is defined in (3.9). The spectral properties of the

corresponding integral operator defined by (3.10) is investigated below. The simple, and frequently used composite Simpson's rule [14] is employed to approximate the one-dimensional integral operator, yielding the finite dimensional eigenvalue problem stated in (3.12). In the numerical examples below, the number of quadrature points is set to $N = 401$.

The one-dimensional kernel function $g(x)$ defined in (3.11) is shown in Fig. 3 for $B = \{2, 0.2, 0.1\}$. Examples of the corresponding eigenfunctions when $k_0 a = 20$ and $B = 2$ is shown in Fig. 4.

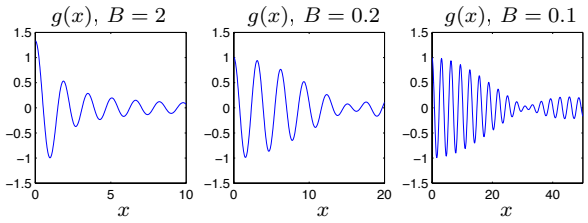

Figure 3: The kernel function $g(x)$ for $B = \{2, 0.2, 0.1\}$.

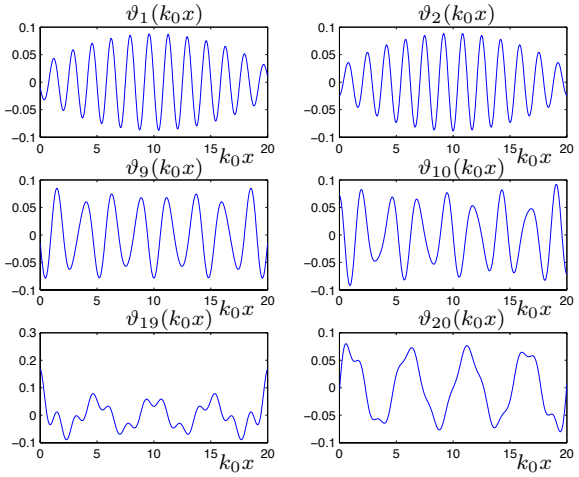

Figure 4: Examples of eigenfunctions $\vartheta_l(k_0x)$ corresponding to the kernel function $g(x)$ for $k_0 a = 20$, $B = 2$ and $l = \{1, 2, 9, 10, 19, 20\}$.

The eigenvalues of the integral operator in (3.10) is shown in Fig. 5 for $B = 2$ and $k_0 a = \{1, 2, 5, 10, 20, 50, 100\}$. The upper part of Fig. 5 shows the eigenvalues in decreasing order (counting multiplicity). The resolution limit is determined by the number of useful eigenfunctions, and is hence given approximately by the sharp "knee", or "threshold", at which the eigenvalues starts to drop off in rapid exponential decay.

Define the resolution limit based on l useful eigenfunctions by

$$\mathcal{R}_{\lambda_{\min}} = \frac{a}{\lambda_{\min}} \frac{1}{l} = \frac{k_0 a}{2\pi} (1 + \frac{B}{2}) \frac{1}{l} \tag{5.1}$$

in dimensionless fractions of the minimum wavelength $\lambda_{\min}$. Note that $k_0 = \omega_0/c$ denotes the wave number corresponding to the center frequency ω_0, and the minimum

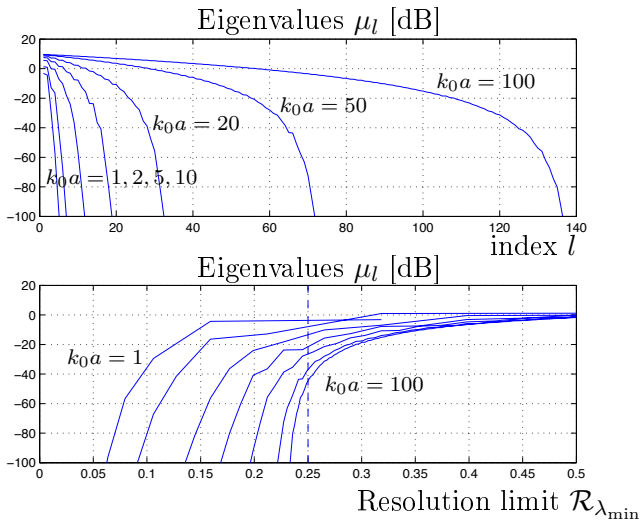

Figure 5: Upper part: Eigenvalues μ_l as a function of index (counting multiplicity) corresponding to the kernel function $g(x)$. Lower part: Eigenvalues μ_l as a function of resolution limit $\mathcal{R}_{\lambda_{\min}}$ in fractions of the minimum wavelength $\lambda_{\min}$. Here, $B = 2$ and $k_0a = \{1, 2, 5, 10, 20, 50, 100\}$.

wavelength is $\lambda_{\min} = \lambda_0/(1 + B/2)$. The lower part of Fig. 5 shows the eigenvalues μ_l as a function of the resolution limit $\mathcal{R}_{\lambda_{\min}}$ defined in (5.1). As can be seen in Fig. 5, the resolution limit approaches $\Delta x/\lambda_{\min} = 1/4$ as $k_0a \to \infty$ and $B = 2$, as predicted by the asymptotic analysis in (3.19).

In Fig. 6 is shown the eigenvalues of the integral operator in (3.10) for $k_0a = 10$ and $B = \{0.1, 0.2, 0.5, 1, 2\}$. Note that the "staircase" shape of these curves are quite natural since the eigenvalues become double as k_0a is getting large, *cf.*, the asymptotic analysis in section 3.3.

In Fig. 4 is shown a selection of useful eigenfunctions within the resolution limit for $k_0a = 20$ and $B = 2$. It is concluded from Fig. 5 that a resolution limit of $\mathcal{R}_{\lambda_{\min}} = 0.25$ corresponds approximately to $l = 25$ linearly independent eigenfunctions. To demonstrate the actual resolution capability versus the predicted $\mathcal{R}_{\lambda_{\min}}$, an eigenfunction expansion of two closely spaced impulse functions $\delta(x-x_1)+\delta(x-x_2)$ is carried out. In Fig. 7 is shown an expansion using the first 25 eigenfunctions. The distance between the impulses are $d = |x_1 - x_2| = \lambda_{\min}\{0.5, 0.4, 0.3\}$.

5.2 Two-dimensional inverse scattering

Consider the two-dimensional inverse scattering problem described in section 4. The dimensionless Fisher information is defined in (4.21) and decomposed in a Fourier series in (4.22) and (4.23). The spectral properties of the corresponding integral operator defined by (4.24) is investigated below. A numerical scheme is used here where (4.23) is truncated with $|q| \leq Q$ and $|m| \leq 2Q$. The simple, and frequently used composite Simpson's rule [14] is employed to approximate the one-dimensional inte-

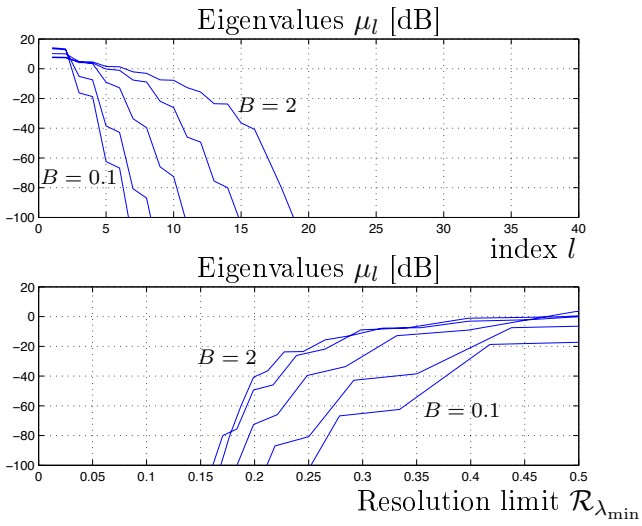

Figure 6: Upper part: Eigenvalues μ_l as a function of index (counting multiplicity) corresponding to the kernel function $g(x)$. Lower lower part: Eigenvalues μ_l as a function of resolution limit $\mathcal{R}_{\lambda_{\min}}$ in fractions of the minimum wavelength $\lambda_{\min}$. Here, $k_0 a = 10$ and $B = \{0.1, 0.2, 0.5, 1, 2\}$.

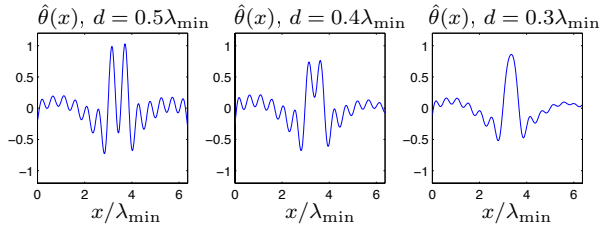

Figure 7: Eigenfunction expansion of two closely spaced impulse functions $\delta(x - x_1) + \delta(x - x_2)$ using the eigenfunctions $\vartheta_l(k_0 x)$ for $l = 1, \ldots, 25$, corresponding approximately to the resolution limit $\mathcal{R}_{\lambda_{\min}} = 0.25$ for $k_0 a = 20$ and $B = 2$. The distance between the impulses are $d = |x_1 - x_2| = \lambda_{\min}\{0.5, 0.4, 0.3\}$.

gral operators in (4.25), yielding the finite dimensional eigenvalue problems stated in (4.28). In the numerical examples below, the Fourier series truncation is set to $Q = 40$ and the number of radial quadrature points is $N = 31$. Hence, there is a total of 2511 eigenvalues (counting multiplicity). In the numerical examples below, the measurement cylinder radius is $b = 1.1a$.

Consider the narrowband case $B \to 0$, which is easily accounted for by putting $\nu = 1$, $\mathrm{d}\nu = B$ and neglecting the integral over ν in (4.23). Let λ_0 denote the wavelength and $k_0 = 2\pi/\lambda_0$ the wave number. The eigenvalues of the integral operator in (4.24) is shown in Fig. 8 for $k_0 a = 2\pi\{1, 2, 4, 8\}$. The upper part of Fig. 8 shows the eigenvalues in decreasing order (counting multiplicity). As with the previous one-dimensional example, the resolution limit is given here approximately by the sharp "knee", or "threshold", at which the eigenvalues starts to drop off in rapid exponential decay.

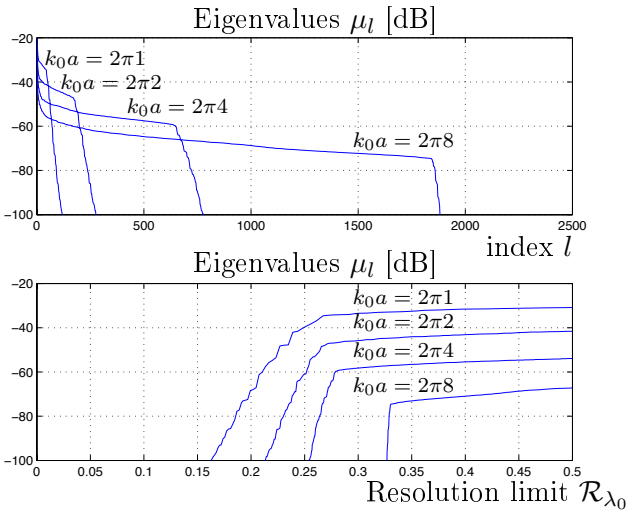

Figure 8: Upper part: Eigenvalues μ_l as a function of index (counting multiplicity) corresponding to the Fisher information kernel for a two-dimensional circular domain. Lower part: Eigenvalues μ_l as a function of resolution limit $\mathcal{R}_{\lambda_0}$ in fractions of the wavelength λ_0. Here, $B = 0$ (narrowband case) and $k_0a = 2\pi\{1, 2, 4, 8\}$.

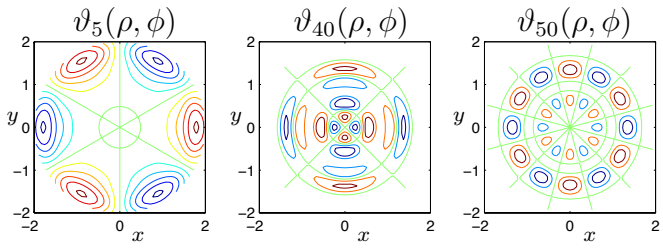

Figure 9: A selection of useful eigenfunctions $\vartheta_l(\rho, \phi)$ with $l = \{5, 40, 50\}$ within the resolution limit ($l = 180$) for $k_0a = 2\pi2$, corresponding to the Fisher information operator for a two-dimensional circular domain. The cartesian x and y axes shown are normalized to the wavelength and the radius of the circular domain is $a = 2\lambda_0$.

The resolution limit may be further quantified as follows. A dimensionless measure of the cylinder cross-section area is $A_{\lambda_0} = \pi(\frac{a}{\lambda_0})^2 = \pi(\frac{k_0a}{2\pi})^2$ and the corresponding resolution limit based on l useful eigenfunctions is defined by

$$\mathcal{R}_{\lambda_0} = \sqrt{\frac{A_{\lambda_0}}{l}} = \sqrt{\frac{(k_0a)^2/4\pi}{l}} \tag{5.2}$$

in dimensionless fractions of the wavelength λ_0. The lower part of Fig. 8 shows the eigenvalues μ_l as a function of the resolution limit $\mathcal{R}_{\lambda_0}$ defined in (5.2).

In Fig. 9 is shown a selection of useful eigenfunctions with various spatial variability, chosen within the resolution limit for $k_0a = 2\pi2$. It is concluded from Fig. 8 that a resolution limit of $\mathcal{R}_{\lambda_0} = 0.27$ corresponds approximately to $l = 180$ linearly independent eigenfunctions.

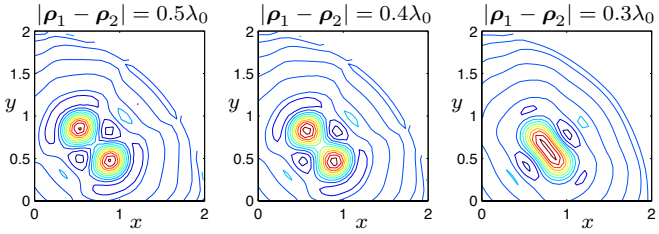

Figure 10: Eigenfunction expansion of two closely spaced impulse functions $\delta(\boldsymbol{\rho} - \boldsymbol{\rho}_1) + \delta(\boldsymbol{\rho} - \boldsymbol{\rho}_2)$ using the eigenfunctions $\vartheta_l(\rho, \phi)$ for $l = 1, \ldots, 180$, corresponding approximately to the resolution limit for $k_0 a = 2\pi 2$. The distance between the impulses are $|\boldsymbol{\rho}_1 - \boldsymbol{\rho}_2| = \lambda_0\{0.5, 0.4, 0.3\}$. The cartesian x and y axes shown are normalized to the wavelength and the radius of the circular domain is $a = 2\lambda_0$.

To demonstrate the actual resolution capability versus the predicted $\mathcal{R}_{\lambda_0}$, an eigenfunction expansion of two closely spaced impulse functions $\delta(\boldsymbol{\rho}-\boldsymbol{\rho}_1)+\delta(\boldsymbol{\rho}-\boldsymbol{\rho}_2)$ is carried out. In Fig. 10 is shown an expansion using the first 180 eigenfunctions. The distance between the impulses is $d = |\boldsymbol{\rho}_1 - \boldsymbol{\rho}_2| = \lambda_0\{0.5, 0.4, 0.3\}$. This eigenfunction expansion may be used to quantify the minimum resolvable distance between two small and closely spaced objects. The numerical examples verify the rather coarse definitions (5.1) and (5.2) with reasonable precision.

6 Summary

The Fisher information integral operator has been defined by using a variational formulation and Fréchet derivatives with a specific application to inverse scattering problems. The spectral decomposition of this compact and self-adjoint operator contains all the essential information about the invertability and the resolution limit for a weak scattering inverse problem, without having to resort to any particular assumptions about the size, orientation and positions of discrete image pixels, etc. It has been illustrated how the integral kernels can be calculated explicitely for some generic one- and two-dimensional inverse scattering problems, and that the related eigenvalue problems can be solved efficiently by using suitable quadrature methods for numerical integration. Moreover, the potential for future research is that the essential eigenfunctions which are obtained from the spectral analysis, will constitute a suitable global basis for optimization and can hence be used with the gradient based inversion algorithms. The future potential is the possibility of unifying the sensitivity and resolution analysis, the regularization, the preconditioning and the inversion algorithm by using one single concept.

Acknowledgement

The authors gratefully acknowledge the financial support by the Swedish Research Council.

References

[1] G. B. Arfken and H. J. Weber. *Mathematical Methods for Physicists.* Academic Press, New York, fifth edition, 2001.

[2] M. Bertero. Linear inverse and ill–posed problems. *Advances in electronics and electron physics*, **75**, 1–120, 1989.

[3] M. Cheney and D. Isaacson. Issues in electrical impedance imaging. *IEEE Computational Science & Engineering*, pages 53–62, 1995.

[4] S. L. Collier. Fisher information for a complex Gaussian random variable: Beamforming applications for wave propagation in a random medium. *IEEE Trans. Signal Process.*, **53**(11), 4236–4248, November 2005.

[5] A. Dogandzic and A. Nehorai. Cramér–Rao bounds for estimating range, velocity, and direction with an active array. *IEEE Trans. Signal Process.*, **49**(6), 1122–1137, June 2001.

[6] A. Fhager, P. Hashemzadeh, and M. Persson. Reconstruction quality and spectral content of an electromagnetic time-domain inversion algorithm. *IEEE Trans. Biomed. Eng.*, **53**(8), 1594–1604, August 2006.

[7] M. Gustafsson and S. He. An optimization approach to two-dimensional time domain electromagnetic inverse problems. *Radio Sci.*, **35**(2), 525–536, 2000.

[8] M. Gustafsson and S. Nordebo. Cramér–Rao lower bounds for inverse scattering problems of multilayer structures. *Inverse Problems*, **22**, 1359–1380, 2006.

[9] J. Kaipio and E. Somersalo. *Statistical and computational inverse problems.* Springer-Verlag, New York, 2005.

[10] S. M. Kay. *Fundamentals of Statistical Signal Processing, Estimation Theory.* Prentice-Hall, Inc., NJ, 1993.

[11] A. Kirsch. *An Introduction to the Mathematical Theory of Inverse Problems.* Springer-Verlag, New York, 1996.

[12] C. H. Knapp and G. C. Carter. The generalized correlation method for estimation of time delay. *IEEE Trans. Acoustics, Speech, and Signal Process.*, **ASSP-24**(4), 320–327, 1976.

[13] P. Kosmas and C. Rappaport. A FDTD-based time reversal for microwave breast cancer detection – localization in three dimensions. *IEEE Trans. Microwave Theory Tech.*, **54**, 1921–1927, apr 2006.

[14] R. Kress. *Linear Integral Equations.* Springer-Verlag, Berlin Heidelberg, second edition, 1999.

[15] K. S. Miller. *Complex Stochastic Processes.* Addison–Wesley Publishing Company, Inc., 1974.

[16] P. S. Naidu and A. Buvaneswari. A study of Cramér–Rao bounds on object shape parameters from scattered field. *IEEE Trans. Signal Process.*, **47**(5), 1478–1481, May 1999.

[17] S. Nordebo, A. Fhager, M. Gustafsson, and M. Persson. A systematic approach to robust preconditioning for gradient based inverse scattering algorithms. *Inverse Problems*, **24**(2), 025027, 2008.

[18] S. Nordebo, M. Gustafsson, and B. Nilsson. Fisher information analysis for two-dimensional microwave tomography. *Inverse Problems*, **23**, 859–877, 2007.

[19] S. Nordebo, M. Gustafsson, and K. Persson. Sensitivity analysis for antenna near-field imaging. *IEEE Trans. Signal Process.*, **55**(1), 94–101, January 2007.

[20] S. Nordebo and M. Gustafsson. Statistical signal analysis for the inverse source problem of electromagnetics. *IEEE Trans. Signal Process.*, **54**(6), 2357–2361, June 2006.

[21] R. Pierri, A. Liseno, and F. Soldovieri. Shape reconstruction from PO multifrequency scattered fields via the singular value decomposition approach. *IEEE Trans. Antennas Propagat.*, **49**(9), 1333–1343, September 2001.

[22] J. G. Proakis. *Digital Communications.* McGraw-Hill, third edition, 1995.

[23] W. Rudin. *Functional analysis.* International series in pure and applied mathematics. McGraw-Hill, New York, 1991.

[24] D. Slepian, H. O. Pollak, and H. J. Landau. Prolate spheriodal wave functions, Fourier analysis and uncertainty, I–II. *Bell System Tech. J.*, **40**, 43–84, 1961.

[25] S. T. Smith. Statistical resolution limits and the complexified Cramér–Rao bound. *IEEE Trans. Signal Process.*, **53**(5), 1597–1609, May 2005.

[26] A. Tarantola. *Inverse problem theory and methods for model parameter estimation.* Society for Industrial and Applied Mathematics, Philadelphia, 2005.

[27] G. A. Tsihirintzis and A. J. Devaney. Maximum likelihood estimation of object location in diffraction tomography, Part II; strongly scattering objects. *IEEE Trans. Signal Process.*, **39**(6), 1466–1470, June 1991.

[28] H. L. Van Trees. *Detection, Estimation and Modulation Theory, part I.* John Wiley & Sons, Inc., New York, 1968.